Since January 2020 Elsevier has created a COVID-19 resource centre with free information in English and Mandarin on the novel coronavirus COVID-19. The COVID-19 resource centre is hosted on Elsevier Connect, the company's public news and information website.

Chemical Engineering Journal 418 (2021) 129368

Contents lists available at ScienceDirect

Chemical Engineering Journal

journal homepage: www.elsevier.com/locate/cej

One-step vapor deposition of fluorinated polycationic coating to fabricate antifouling and anti-infective textile against drug-resistant bacteria and viruses

Qing Song [a,b,1,*], Ruixiang Zhao [a,1], Tong Liu [c,1], Lingling Gao [a], Cuicui Su [d], Yumin Ye [d,*], Siew Yin Chan [a], Xinyue Liu [a], Ke Wang [a], Peng Li [a,*], Wei Huang [a,b]

[a] Ningbo Institute, Frontiers Science Center for Flexible Electronics (FSCFE), Xi'an Institute of Flexible Electronics (IFE) and Xi'an Institute of Biomedical Materials & Engineering (IBME), Northwestern Polytechnical University, 127 West Youyi Road, Xi'an 710072, China
[b] Key Laboratory for Organic Electronics and Information Displays, Institute of Advanced Materials (IAM), Nanjing University of Posts & Telecommunications, 9 Wenyuan Road, Nanjing 210023, China
[c] Sichuan Tengli Agri-Tech Co. Ltd., Deyang 618200, China
[d] Department of Materials Science and Engineering, Faculty of Materials Science and Chemical Engineering, Ningbo University, Ningbo 315211, China

ARTICLE INFO

Keywords:
Initiated chemical vapor deposition (iCVD)
Fluorinated hydrophobic polymer
Polycationic coating
Antifouling
Antibacterial
Antiviral

ABSTRACT

The ongoing pandemic caused by the novel coronavirus has turned out to be one of the biggest threats to the world, and the increase of drug-resistant bacterial strains also threatens the human health. Hence, there is an urgent need to develop novel anti-infective materials with broad-spectrum anti-pathogenic activity. In the present study, a fluorinated polycationic coating was synthesized on a hydrophilic and negatively charged polyester textile via one-step initiated chemical vapor deposition of poly(dimethyl amino methyl styrene-*co*-1H,1H,2H,2H-perfluorodecyl acrylate) (P(DMAMS-*co*-PFDA), PDP). The surface characterization results of SEM, FTIR, and EDX demonstrated the successful synthesis of PDP coating. Contact angle analysis revealed that PDP coating endowed the polyester textile with the hydrophobicity against the attachment of different aqueous foulants such as blood, coffee, and milk, as well as the oleophobicity against paraffin oil. Zeta potential analysis demonstrated that the PDP coating enabled a transformation of negative charge to positive charge on the surface of polyester textile. The PDP coating exhibited excellent contact-killing activity against both gram-negative *Escherichia coli* and gram-positive methicillin-resistant *Staphylococcus aureus*, with the killing efficiency of approximate 99.9%. In addition, the antiviral capacity of PDP was determined by a green fluorescence protein (GFP) expression-based method using lentivirus-EGFP as a virus model. The PDP coating inactivated the negatively charged lentivirus-EGFP effectively. Moreover, the coating showed good biocompatibility toward mouse NIH 3T3 fibroblast cells. All the above properties demonstrated that PDP would be a promising anti-pathogenic polymeric coating with wide applications in medicine, hygiene, hospital, etc., to control the bacterial and viral transmission and infection.

1. Introduction

The discovery of antibiotics is a major milestone in the field of medicine and health care, since antibiotics efficiently inhibit bacterial infection and significantly increase human lifespan. However, with the increasing resistance of bacteria to antibiotics due to the excessive and inappropriate use, the efficacy of antibiotics is generally declining [1,2]. Some common pathogens are becoming drug-resistant "superbug", such as methicillin-resistant *Staphylococcus aureus* (MRSA), vancomycin-resistant *Enterococcus*, multidrug-resistant *Pseudomonas aeruginosa*, etc. [3,4]. In addition, the infectious diseases caused by viruses have been threatening human health, such as Ebola virus, human immunodeficiency virus (HIV), hepatitis virus, influenza virus, etc. [5]. Since December 2019, the novel coronavirus (SARS-CoV-2) [6–11] has caused millions of human deaths around the world. Therefore, the antibacterial and antiviral materials for preventing and controlling pathogenic

* Corresponding authors at: Ningbo Institute, Frontiers Science Center for Flexible Electronics (FSCFE), Xi'an Institute of Flexible Electronics (IFE) and Xi'an Institute of Biomedical Materials & Engineering (IBME), Northwestern Polytechnical University, 127 West Youyi Road, Xi'an 710072, China (Q. Song).
E-mail addresses: iamqsong@nwpu.edu.cn (Q. Song), yeyumin@nbu.edu.cn (Y. Ye), iampli@nwpu.edu.cn (P. Li).
[1] These authors contributed to this work equally.

https://doi.org/10.1016/j.cej.2021.129368
Received 16 December 2020; Received in revised form 27 February 2021; Accepted 10 March 2021
Available online 16 March 2021

infections have attracted worldwide attention.

Infectious pathogens spread when liquids containing bacteria and viruses settle onto surfaces and subsequently are touched by people. This could be prevented if the surfaces are coated with antimicrobial polymers. Generally, the antimicrobial polymeric coatings are designed based on two strategies: antifouling and killing [12–16]. The prevention of contaminant adhesion on surfaces could efficiently inhibit pathogen infections [17]. The hydrophobic coatings showed liquid-repelling activity [18,19], and thus could inhibit the adhesion of microbes from the contaminated liquid and avoid the subsequent infections. The fluorine-containing polymeric coatings possessed hydrophobicity due to its low surface energy, which could resist the attachment of liquid pollutant [20]. Although the antifouling surfaces can reduce the risk of pathogenic infections, the attachment of pathogenic microbes on the surfaces cannot be avoided under the action of external forces. Therefore, the contact-killing performance against microbes is also essential for antimicrobial coatings [21].

In nature, most bacteria and viruses are negatively charged at neutral pH [22,23], and therefore positively charged materials are easy to interact with most bacteria and viruses, and subsequently inactivate bacteria and viruses by destroying their structures [24]. The cationic organic chemicals such as quaternary ammonium salts are widely studied in the antibacterial and antiviral field [25]. Some cationic monomers are harmful to human body. However, the polymerization of cationic monomers not only increases the density of functional groups, but also reduces the toxicity of monomers. Moreover, the polycationic coatings endowed various surfaces with antimicrobial activity without the alteration of the bulk property. By now, most antimicrobial polycationic coatings are focused on bacteria [26,27]. A study about fluorine-containing polycationic coatings on textiles with antifouling and antibacterial dual-function only aimed at bacteria [28]. There were only a few studies reported in the area of polycationic coatings against both bacteria and viruses [29,30], and these studies only investigated the contact-killing activity, but did not mention the antifouling behaviors of antimicrobial coatings. Therefore, this study was aimed to investigate the fluorine-containing polycationic coatings with antifouling and contact-killing dual activities against both bacteria and viruses.

In addition, most polycationic coatings immobilized on surfaces require multi-step solution-based methods and solvents. The solvent treatment may not fit solvent-sensitive substrates and possibly induce the harmful impurities. Initiated chemical vapor deposition (iCVD) is a dry coating technology based on gas-to-surface reaction, and able to avoid the complicated multi-step processes and bypass the use of any solvent [31,32]. Compared with other coating techniques such as electrospinning [33,34], iCVD is more advantageous for cases that need delicate modification of nanometer-sized pores and require uniform conformal coatings in complex geometries such as porous textiles [35] and electronic devices [36]. In our previous study, we coated the cationic poly(dimethyl amino methyl styrene) (PDMAMS) via iCVD in various polymer structures such as crosslinking [35], grafting [37], and graded layers [27] on surfaces of textile, medical catheter, and polystyrene slide, endowing the surfaces with potent bactericidal efficacy. We found that the hydrophilic poly(vinyl pyrrolidone)-enriched PDMAMS surface possessed the contact-killing and pH-responsive antifouling activities against bacteria [27]. While, in the present study, we investigated the liquid-repelling and antimicrobial activities of a hydrophobic polycationic coating composed of the fluorine-containing 1H,1H,2H,2H-perfluorodecyl acrylate (PFDA) and DMAMS via one-step iCVD, aiming to facilely fabricate a self-cleaning textile surface that could combat the transmission and infection of drug-resistant bacteria and viruses (Fig. 1).

2. Material and methods

2.1. Material

Dimethyl amino methyl styrene (DMAMS, 95%) was purchased from Acros Organics (USA). 1H,1H,2H,2H-perfluorodecyl acrylate (PFDA, 98%) and *tert*-butyl peroxide (TBP, 98%) were purchased from Adamas

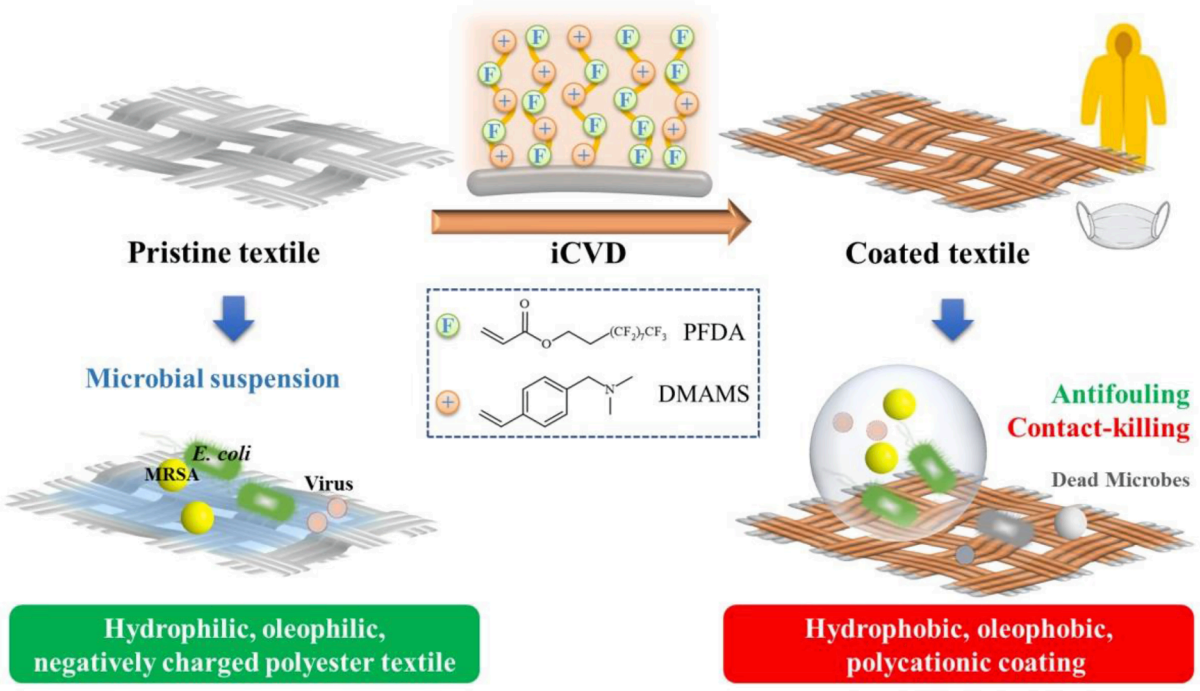

Fig. 1. The one-step iCVD of the cationic and fluorinated P(DMAMS-*co*-PFDA) (PDP) coating on the surface of hydrophilic polyester textile. Compared with the pristine textile, the coating endowed the textile with hydrophobicity, oleophobicity, and thus antifouling ability; the coating was positively charged and inactivated the negatively charged bacteria and viruses on contact. The facile iCVD process can apply the potent antifouling, antibacterial, and antiviral coating to the anti-infective field.

(China). The DMAMS and PFDA monomers were vacuum purified prior to use to remove volatile impurities. Silicon wafer and polyester textile were used as substrates. Silicon wafer was used as a reference substrate for coating characterization. *Escherichia coli* (*E. coli*, ATCC 25922) and methicillin-resistant *Staphylococcus aureus* (MRSA, ATCC BAA40) were obtained from American Type Culture Collection (ATCC, USA). Luria-Bertani (LB) broth and agar, Dulbecco's Modified Eagle Medium (DMEM), and newborn calf serum (NCB) were obtained from Sigma-Aldrich (USA). Phosphate Buffered Saline (PBS) was purchased from Biosharp (China). The Alamar Blue Cell Viability reagent and LIVE/DEAD Viability/Cytotoxicity Kit for mammalian cells were purchased from Thermo Fisher Scientific (USA).

2.2. Coating fabrication via iCVD

The schematic diagram of an iCVD system is shown in Fig. 2. The vapor deposition process was performed in a 25 cm diameter custom-built reactor equipped with parallelly arranged nichrome filaments (Ni80/Cr20, Goodfellow) that were heated to 280 °C to thermally decompose the initiator TBP and generate radicals. The filament temperature was measured by a K-type thermocouple (Omega) that connected to a filament wire. The substrates were placed on a stainless-steel stage quenched by circulating water and kept at 40 °C. To prevent condensation of monomers, the temperature of the pipelines that connected the monomer jars to reactor was set at 80 °C, and that of reactor wall was kept at 60 °C. During deposition, monomers PFDA and DMAMS, and initiator TBP were evaporated at 80 °C, 68 °C, and 30 °C, respectively, and flowed into the reactor. The flow rate of each precursor was controlled by a needle valve (Swagelok). The vacuum was achieved by a dry vacuum pump (Edwards iH-80). The reactor pressure was kept constant at 0.3 Torr, which was measured by a capacitance manometer (MKS Baratron) and controlled by a butterfly throttling valve (MKS). The coating growth on the reference silicon substrate was monitored in situ using an interferometry with a 633 nm He-Ne laser. The detailed deposition conditions are listed in Table 1.

2.3. Characterizations of the coatings

Fourier transform infrared (FTIR) spectra of the coatings on the reference silicon wafers were measured using a Nicolet 6700 FTIR spectrometer equipped with a DTGS detector under transmission mode. The surface morphology and elemental analysis were implemented by scanning electron microscope (SEM, FEI, Verios G4) and energy-dispersive X-ray (EDX, Thermo Scientific NORAN System 7).

Table 1
Deposition conditions of PDMAMS, PPFDA, and PDP coatings.

Sample	Pressure (Torr)	Flow rate (sccm)		
		DMAMS	PFDA	TBP
PDMAMS	0.3	2	/	0.6
PPFDA	0.3	/	0.2	0.6
PDP	0.3	2	0.2	0.6

2.4. Antifouling test

The liquid repellency of the PDP coating was investigated with diverse liquid foulants. The different solutions including blood (New Zealand rabbit), paraffin oil (GHTECH, China), honey, pH calibration buffer solutions at pH 4.00, pH 6.86, pH 9.18, coffee, milk were dropped on the surface of the pristine and PDP-coated textiles, and images were taken by a Canon digital camera. Contact angles of water and paraffin oil on samples were measured using a contact angle goniometer (Kruss DSA 25, Germany).

2.5. Coating stability

The coating stability was determined through the comparison of water contact angles before and after abrasion resistance and washing durability tests. Abrasion resistance of PDP coated textiles was tested by sliding a nominal load of 3.15 kPa on samples for 20 cm in length. The procedure was repeated for 1000 cycles. Subsequently, the washing durability of the textiles was tested as following. The textiles were put into a beaker (200 mL) with 50 steel balls (diameter = 6 mm) in deionized water, shaken at 200 rpm for 10 min, and then air dried, which was repeated for 30 cycles. Finally, the water contact angles of the textiles were measured (Kruss DSA 100, Germany).

2.6. Zeta potential measurement of textiles and microbes

The zeta potential values of the pristine textile, PPFDA and PDP coated textiles were determined in 0.0007 M PBS (pH 7.1) using a solid surface zeta potential analyzer (Anton Paar Sur PASS 3). The zeta potential values of gram-positive bacteria MRSA (2.0×10^7 CFU/mL),

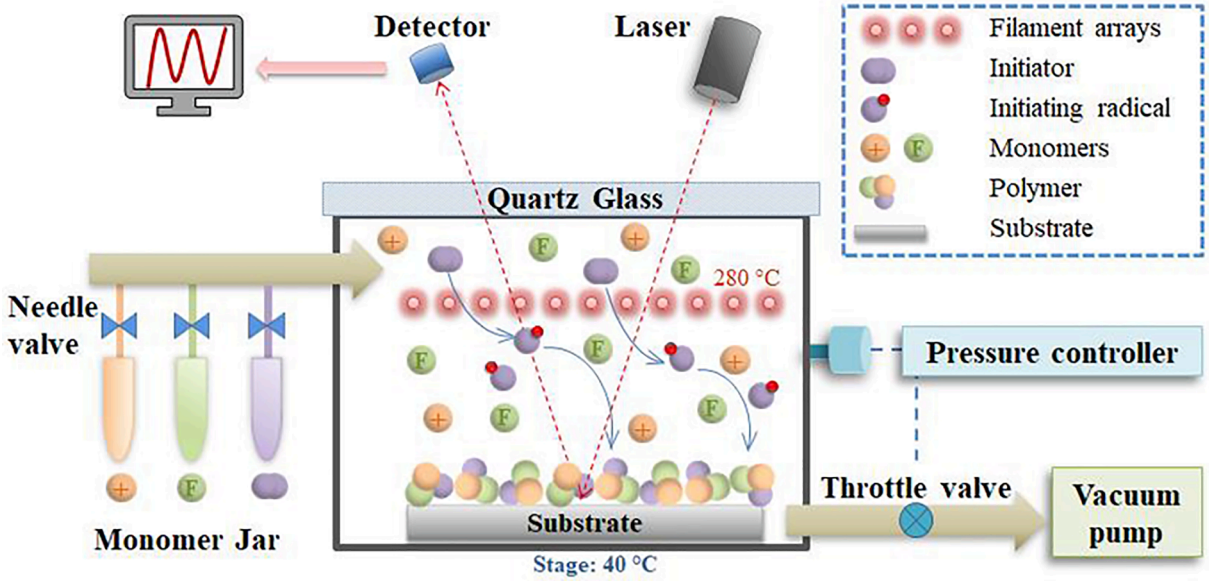

Fig. 2. A schematic diagram of an iCVD system.

gram-negative bacteria *E. coli* (2.8×10^7 CFU/mL), and lentivirus-EGFP (1.0×10^6 TU/mL) were measured by Zetasizer Nano ZS (Malvern, UK) in 0.01 M PBS (pH 7.1).

2.7. Antibacterial test

The antibacterial activity of the samples was evaluated according to a bacterial contact-killing assay. One mL of the bacterial suspension (*E. coli* or MRSA) at mid-log phase was collected by centrifugation, washed three times using PBS (0.01 M), and then diluted to 1×10^7 CFU/mL in PBS. Ten μL of the diluted bacterial working solution was pipetted onto the surface of a pristine or a coated textile (1 cm × 1 cm), and then a glass cover slide was placed over the bacterial solution to ensure the complete contact between the bacteria and the textile, followed by the incubation at 37 °C for 1 h with a relative humidity maintaining above 90% to prevent inoculums from drying. After incubation, the pristine or the coated textile was immerged in 1.0 mL of PBS, and then sonicated for 3 min to re-suspend the live bacterial cells. Afterwards, the retrieved cells were 10-fold diluted to a series of concentrations of bacterial suspensions for agar plating, and then the plates were incubated overnight for CFU counting. The log reduction of *E. coli* or MRSA was calculated using the below equation: log reduction = log (cell counts of pristine textile) – log (cell counts of the coated textile).

Inhibition zone test was conducted as following. Fifty μL of bacterial suspensions (MRSA and *E. coli*) at mid-log growth phase were spread on the LB agar plates. Then, the textile samples including povidone-iodine (PVP-I) soaked textile as a release-killing control, pristine textile, PPFDA and PDP coated textiles (around 1 × 1 cm) were placed on the agar plates and incubated at 37 °C overnight.

The bacterial morphology on textiles was examined under SEM. After bacterial incubation on textiles for 1 h, samples were fixed by 4% paraformaldehyde for 12 h and dehydrated through a series of ethanol solutions with increasing concentrations (25%, 50%, 70%, 90%, 95%, and 100%). Afterwards, the samples were dried by hexamethyldisilazane. Finally, the samples were coated by Au-Pd and observed under SEM (FEI, Verios G4).

2.8. Antiviral test

In order to directly observe the antiviral activity of the PDP coating, the recombinant lentivirus (a single-stranded RNA virus) with enhanced green fluorescence protein (*egfp*) gene was used in this study to infect mouse NIH 3T3 fibroblast cells. If the sample can inactivate the viruses, the cells neither express EGFP nor show green fluorescence after virus infection; if the sample cannot inactivate the viruses, the cells will express EGFP and show green fluorescence. The cells were cultured in DMEM supplemented with 10% (v/v) NCB, 100 μg/mL penicillin, and 100 μg/mL streptomycin, and incubated in a humidified atmosphere containing 5% CO_2 at 37 °C. About 1×10^4 cells were seeded in each well of 48-well tissue-culture polystyrene plate (TCPS) and cultured for 24 h.

For the antiviral test, briefly, 3 μL droplet of lentivirus-EGFP (3.3×10^8 TU/mL in 0.01 M PBS, the multiplicity of infection was 200) was deposited on a textile sample (1 cm × 1 cm) in a well of 24-well TCPS. Then, a plain glass slide was put on the top of the sample and pressed to spread the droplet. After incubation at room temperature for 30 min, the top slide was lifted and 0.5 mL of DMEM medium with NCB was added into each well to suspend the viruses. Then, the virus suspension was collected and subsequently infected mouse NIH 3T3 fibroblast cells with polybrene (1:200). The normal medium was refreshed on the second day. After 3 days, the infected cells were observed under a fluorescence microscope (Evos FL Auto 2, Invitrogen) with a green filter (excitation/emission: 470/525 nm), and the total cells were observed in a bright field for comparison (Fig. 3).

2.9. Biocompatibility test

The biocompatibility of PDP coating was measured with Alamar Blue and LIVE/DEAD assay. About 1×10^4 mouse NIH 3T3 fibroblast cells were seeded in each well of 24-well TCPS and cultured for 24 h. The pristine textile and PDP coated textile were sterilized under UV irradiation for 1 h, rinsed with sterile deionized water, and put into the wells with the cells for 24 h. Afterwards, the textiles were removed, and the cell viability was measured with Alamar Blue. After stained with dyes from a LIVE/DEAD Viability/Cytotoxicity Kit for mammalian cells, the cellular morphologies were observed under a fluorescence microscope (Evos FL Auto 2, Invitrogen) with the excitation wavelengths of 470 nm and 531 nm for the detection of GPF (green) and RFP (red), respectively.

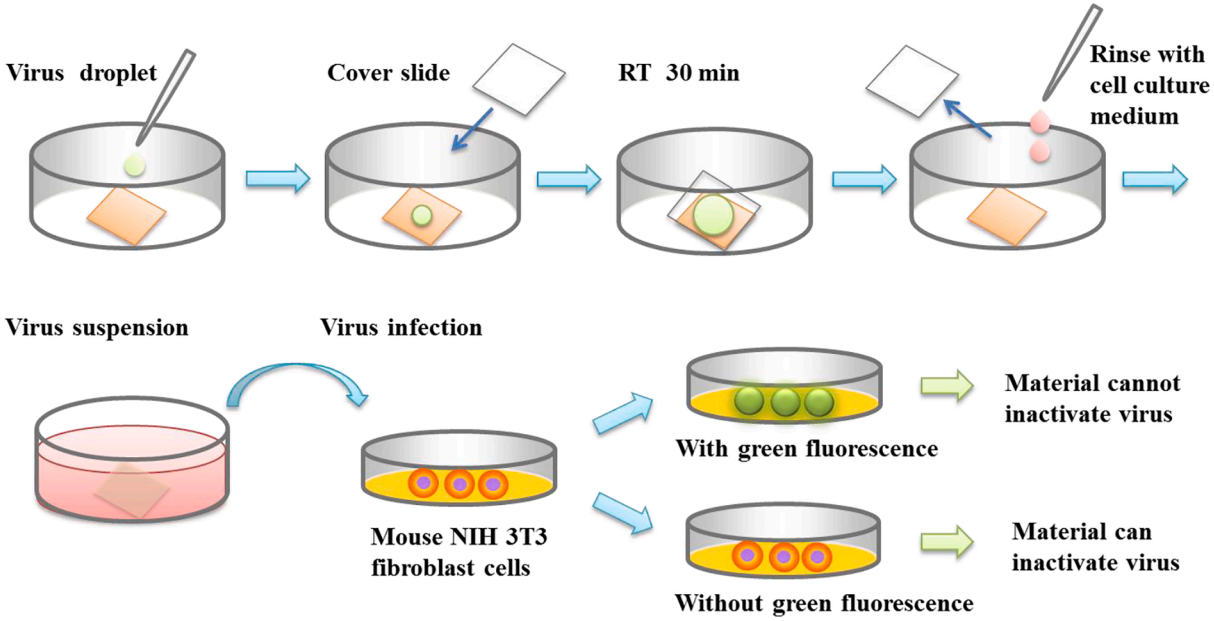

Fig. 3. Procedure for antiviral testing based on lentivirus-EGFP infection assay.

2.10. Statistical analysis

All data were presented as mean value ± standard deviation, and the statistically significant differences were examined using one-way ANOVA followed by Tukey's HSD test with GraphPad Prism 6 (GraphPad Software, La Jolla). In all statistical evaluations, $p < 0.05$ was considered to be statistically significant.

3. Results and discussion

3.1. Preparation and characterization of PDP coating on textile

The cationic and fluorinated polymeric coating P(DMAMS-*co*-PFDA) (PDP) was fabricated via a one-step iCVD process. The vaporized monomers DMAMS and PFDA, along with the initiator TBP, were fed into the reactor to deposit polymer PDP on the reference silicon wafer and pristine polyester textile. For comparison, homopolymer PDMAMS and PPFDA coatings were also synthesized (Table 1). An approximate 150 nm surface layer is coated on the textile, as shown in the cross section by SEM images (Fig. 4a). FTIR spectra show the chemical compositions of the polymeric coatings (Fig. 4b). In the spectrum of PPFDA, the characteristic peaks are associated with the fluorinated groups, including symmetric and asymmetric -CF_2- stretching (centered at 1205 and 1238 cm^{-1}) and stretching of -CF_2-CF_3 end group (1150 cm^{-1}), and the C = O stretching from the ester group at 1741 cm^{-1} [38]. In the spectrum of PDMAMS, the peaks ranging from 2730 cm^{-1} to 2830 cm^{-1} are attributed to the C–H stretching in the -$N(CH_3)_2$ group of PDMAMS [35]. The spectrum of PDP contains both characteristic peaks of homopolymers PPFDA and PDMAMS. There are small wavelength shifts in PDP compared to the homopolymers due to the peak overlap of chemical groups from PDMAMS and PPFDA. In addition, EDX elemental mapping images (Fig. 4c) show that the elements C, O, N, and F exist in PDP coated textile, with higher intensity of N and F compared with the pristine textile. N and F originate from PDMAMS and PPFDA of PDP coating, respectively. The above results demonstrated that copolymer PDP coating was successfully synthesized on the textile via iCVD.

3.2. Antifouling activity and stability

If the surface repels the adhesion of liquids, the surface could avoid the contamination from the liquids, and therefore, in this study, the liquid repellency of the PDP coating was investigated. As shown in Fig. 5, the PDP coating resists the adhesion of diverse solutions including blood (New Zealand rabbit), paraffin oil, honey, pH calibration buffer solutions at pH 4.00, pH 6.86, pH 9.18, coffee, and milk. On the contrary, the hydrophilic pristine textile completely absorbs most liquids except honey. The above results demonstrated that the PDP coating converted the surface of polyester textile from hydrophilic to hydrophobic, from oleophilic to oleophobic, and thus endowed the surface with antifouling property, which were further verified by the contact angles. At 1 min after attachment of water or paraffin oil drops on the surfaces, the contact angles on the pristine textile, PPFDA and PDP coated samples were 0°, 150°, and 144° for water, and 0°, 151°, and 148° for paraffin oil, respectively. Obviously, PPFDA coating enabled the textile with super-hydrophobicity (>150°) [39,40] and super-oleophobicity (>150°) [41]. The incorporation of DMAMS made the contact angles of PDP slightly lower compared with PPFDA, but the PDP coating kept highly hydrophobic and oleophobic. Hence, the PDP coating could repel the adhesion of various solutions and may prevent the attachment of contaminations including pathogens in the liquids. After abrasion resistance and washing durability tests, the water contact angles of PDP slightly reduced from 144° to 141°, and the small change demonstrated that PDP coating had good stability on the textiles.

3.3. Zeta potential

Most bacteria and viruses are negatively charged at a neutral pH [22,23], and thus the proposed antimicrobial mechanism involves electrostatic interaction between the positively charged coating and the negatively charged bacteria and viruses. Here, zeta potential values were measured to investigate electrostatic interaction between the PDP coated textile and the microbes (Fig. 6). The zeta potential values of pristine and PPFDA coated textiles were −20.6 ± 0.7 mV and − 19.5 ± 0.2 mV, respectively, while the PDP coated textile had a positive value

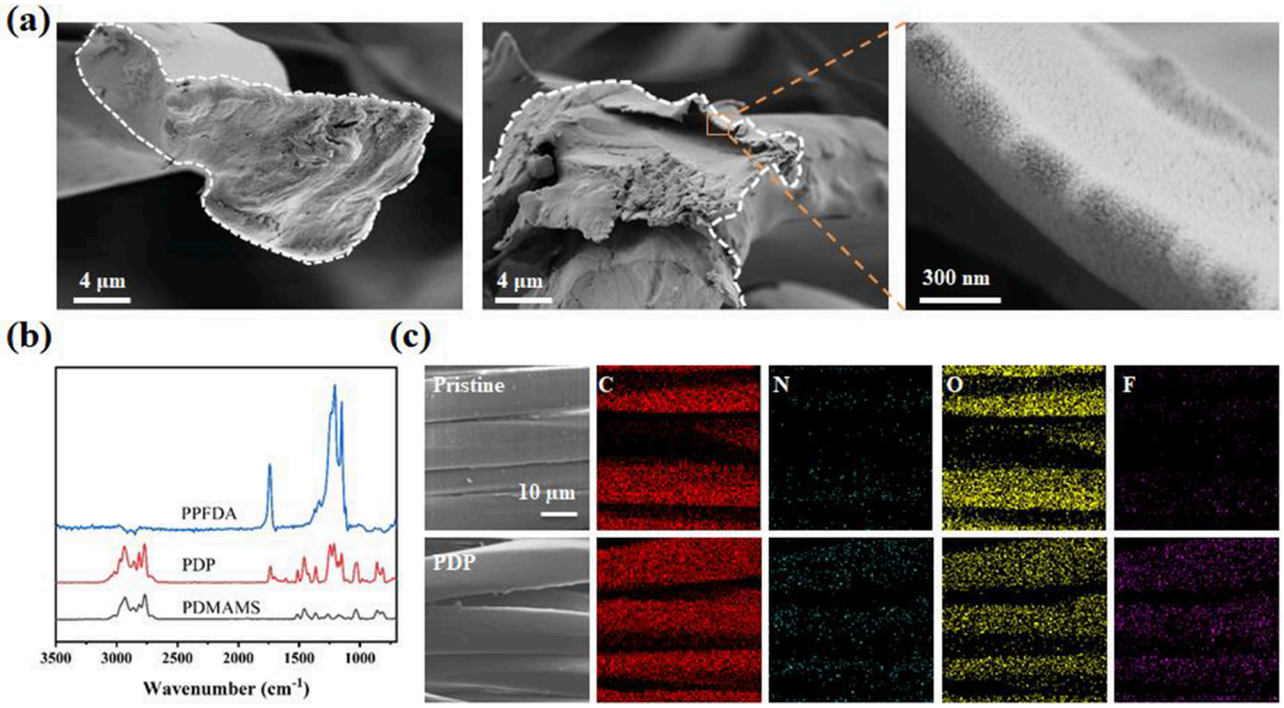

Fig. 4. (a) SEM images of the cross section of pristine textile fiber and PDP coating on the textile fiber. (b) FTIR spectra of PPFDA, PDP, and PDMAMS on the reference silicon wafer surface. (c) EDX elemental mapping of pristine textile and PDP coated textile.

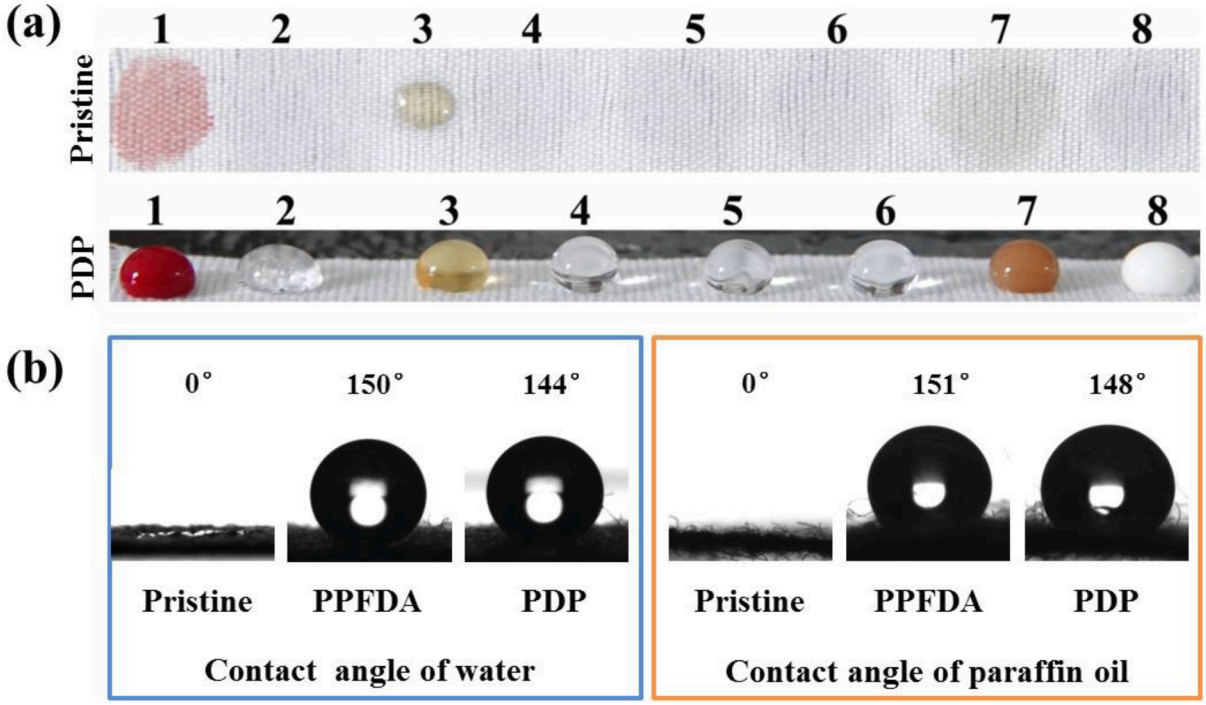

Fig. 5. (a) PDP coating repels the adhesion of liquid drops including (1) blood, (2) paraffin oil, (3) honey, pH calibration buffer solutions at (4) pH 4.00, (5) pH 6.86, (6) pH 9.18, (7) coffee, and (8) milk, while the pristine polyester textile absorbs most liquids. (b) Contact angles of water and paraffin oil on the pristine textile, PPFDA and PDP coated textiles, demonstrating that PDP coating endowed polyester textile surface with hydrophobicity and oleophobicity.

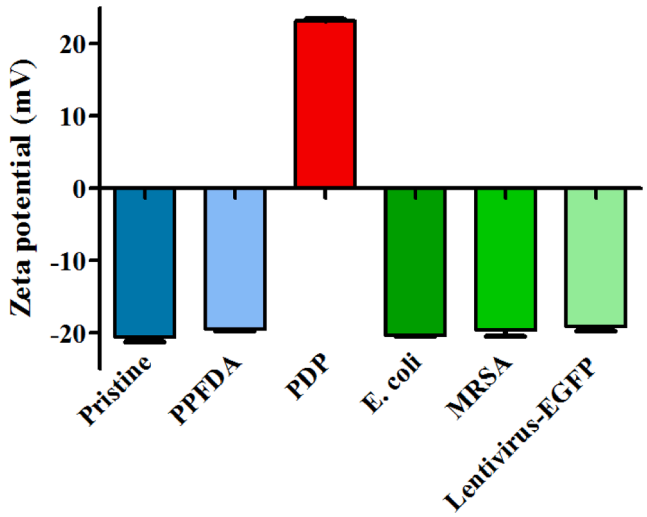

Fig. 6. Zeta potentials of the pristine polyester textile, PPFDA and PDP coated textiles, gram-negative *E. coli*, gram-positive MRSA, and lentivirus-EGFP. The pristine polyester and PPFDA coated textiles were negatively charged. PDP coated textile was positively charged with the surface potential of + 23.2 mV. On the other hand, the zeta potentials of the bacteria and virus are negative.

of + 23.2 ± 0.2 mV. The PDP coating enabled a transformation of charges on the surface of polyester textile, from negatively charged to positively charged, which was because of the cationic DMAMS (pKa ≈ 8.5) [35,42]. For the microbes in this study, the zeta potential values of gram-negative *E. coli*, gram-positive MRSA, and lentivirus-EGFP were −20.3 ± 0.2,−19.6 ± 0.8, and −19.1 ± 0.6, respectively. Obviously, all the microbes in this study were negatively charged. Therefore, the cationic PDP coating could electrostatically attract the negatively charged bacteria and viruses, and subsequently damage the microbial structure, leading to microbial inactivation. The zeta potential effects of antibacterial coatings have been reported previously. Iarikov *et al.* fabricated cationic polyallylamine coatings with the zeta potentials above + 61 mV, which killed gram-negative *P. aeruginosa*, and gram-positive *S. aureus* and *S. epiderimidis* on contact [43]. Choi *et al.* synthesized a cationic copolymer coating with a zeta potential value of + 21.36 mV, which killed gram-negative *E. coli* and gram-positive *Corynebacterium glutamicum* [44]. However, these studies only focused on the antibacterial aspect. Our study was aimed to investigate the zeta potential effects on the contact-killing performance of polycationic coatings against both bacteria and viruses.

3.4. Antibacterial activity

Although the hydrophobic PDP coating resisted the adhesion of liquid droplets, the bacteria would still be likely to attach to the material surfaces due to the external force. In this study, a glass slide was used to cover a bacterial droplet on a textile sample for the complete contact between the bacteria and the textile sample. After 1 h of contact, the bactericidal behavior of PDP coating, along with the PPFDA coating and pristine textile, was examined. As shown in Fig. 7a, the PDP exhibits significantly enhanced antibacterial activity compared with the pristine textile and PPFDA coated textile. In details, the values of log reduction of gram-positive bacteria MRSA and gram-negative bacteria *E. coli* are 2.96 ± 0.05 and 3.23 ± 0.31, respectively, corresponding to 99.89% and 99.94% killing efficiency (Fig. 7b). Although there was no significant difference of antibacterial efficiency between *E. coli* and MRSA, the killing efficiency of PDP against *E. coli* was a little higher than MRSA, which might be resulted from the fact that the hydrophobic groups in PDP could facilitate the penetration of the polycations into the hydrophobic structure of cell wall such as the lipid domains, especially the outer membrane of gram-negative bacteria [28]. Gram-positive bacteria just have a thicker peptidoglycan layer and inner plasma membrane without outer membrane, which may not further promote the interaction between the PDP coating and MRSA [45]. Therefore, the hydrophobic polycationic PDP killed gram-negative *E. coli* a little more

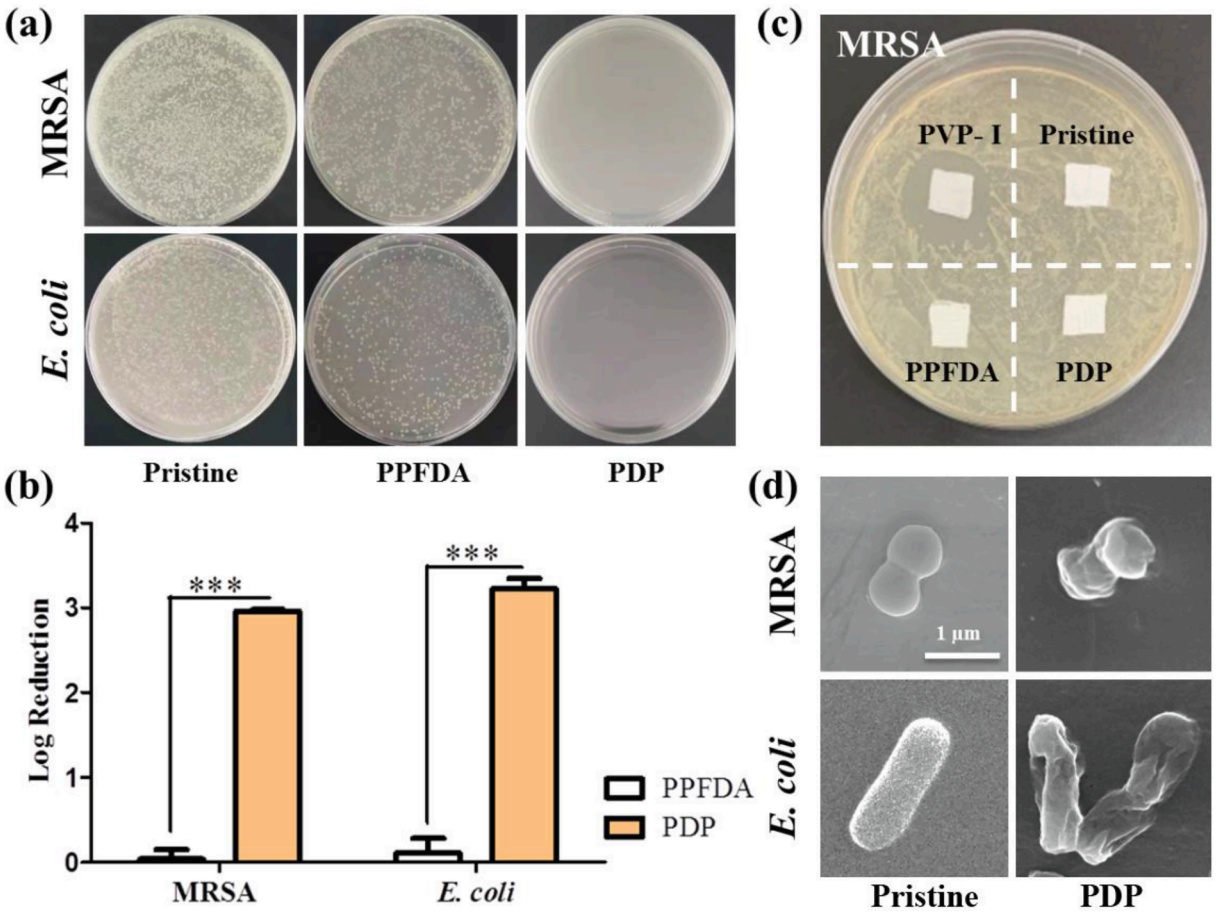

Fig. 7. (a) Antibacterial behavior of pristine polyester textile, PPFDA and PDP coated textiles against gram-positive MRSA and gram-negative *E. coli*. (b) Log reduction of bacterial CFU on contact with PPFDA and PDP coatings (n = 3). (c) Inhibition zones of povidone-iodine (PVP-I) soaked textile as a release-killing control, pristine textile, PPFDA and PDP coated textiles against MRSA. There is no inhibition zone appearing in the PDP group, indicating the PDP coating kills bacteria on contact. (d) Morphology of MRSA and *E. coli* bacterial cells on the surfaces of pristine textile (left, intact bacterial cell envelopes) and PDP coating (right, damaged bacterial cell envelopes) observed by SEM.

efficiently than gram-positive MRSA. However, the major antibacterial mechanism here was attributed to the electrostatic interaction between the cationic PDP coating and the negatively charged bacteria.

Bacterial inhibition zone of textile samples against MRSA (Fig. 7c) shows that the povidone-iodine (PVP-I) soaked textile as a release-killing control has an obvious bacterial inhibition zone based on the release of I. On the contrary, there is no inhibition zone appearing in the pristine, PPFDA, and PDP samples. The result of *E. coli* inhibition zone of textile samples was similar to that of MRSA, indicating that the coatings were stably immobilized on the textile surface and the PDP coating killed bacteria on contact rather than DMAMS releasing.

SEM was used to further observe the bacterial morphology on the PDP coating. In Fig. 7d, MRSA and *E. coli* on the pristine textile show intact profile and smooth cell envelopes. Both MRSA and *E. coli* cells are collapsed on the PDP coated surfaces and the cell envelopes of *E. coli* are seriously damaged, leading to cell death. All the above results indicated that PDP coating possessed potent contact-killing activity against gram-positive drug-resistant MRSA and gram-negative *E. coli*.

3.5. Antiviral activity

With the aim to conveniently observe the antiviral activity of the PDP coating, in this study, we chose the recombinant lentivirus with enhanced green fluorescence protein gene as a virus model. After contact with the samples, the virus suspensions were used to infect mouse NIH 3T3 fibroblast cells (Fig. 3). The fluorescence images in Fig. 8 show that the viruses after contact with the PPFDA coated textile are still able to infect cells and thus cells are appearing green fluorescence, but the amounts of infected cells are obviously less than those of the virus control, indicating that the PPFDA has a certain degree of viral inhibition effect. The lentivirus belongs to the enveloped virus that is protected from outside by a lipid membrane which facilitates virus to enter host cell and protects it from host immune system, such as SARS-CoV-2, SARS coronavirus, Ebola virus, HIV, influenza virus, measles virus, rabies virus and so on [46,47]. The lipid membrane is easy to interact with the hydrophobic groups. The hydrophobic fluorinated groups in the PPFDA coating could penetrate the viral lipid envelope and alter the viral envelope structure. However, PPFDA is negatively charged (Fig. 6), which may hamper the interaction between PPFDA and the negatively charged virus (Fig. 6) due to the electrostatic repulsion. After copolymerization of PFDA and DMAMS, the cationic PDMAMS endowed the PDP coating with the positive charge, which significantly enhanced the electrostatic interaction between the negatively charged lentivirus-EGFP and positively charged PDP. Combined with the hydrophobic interaction between the PPFDA and the viral lipid bilayer and the electrostatic attraction between cationic PDMAMS and the negatively charged virus, the PDP coating damaged the viral structure and therefore exhibited excellent antiviral activity. The results were consistent with previous reports, such as the hydrophobic polycation N, N-dodecyl, methyl-polyethylenimine against enveloped herpes simplex viruses and influenza viruses [48,49].

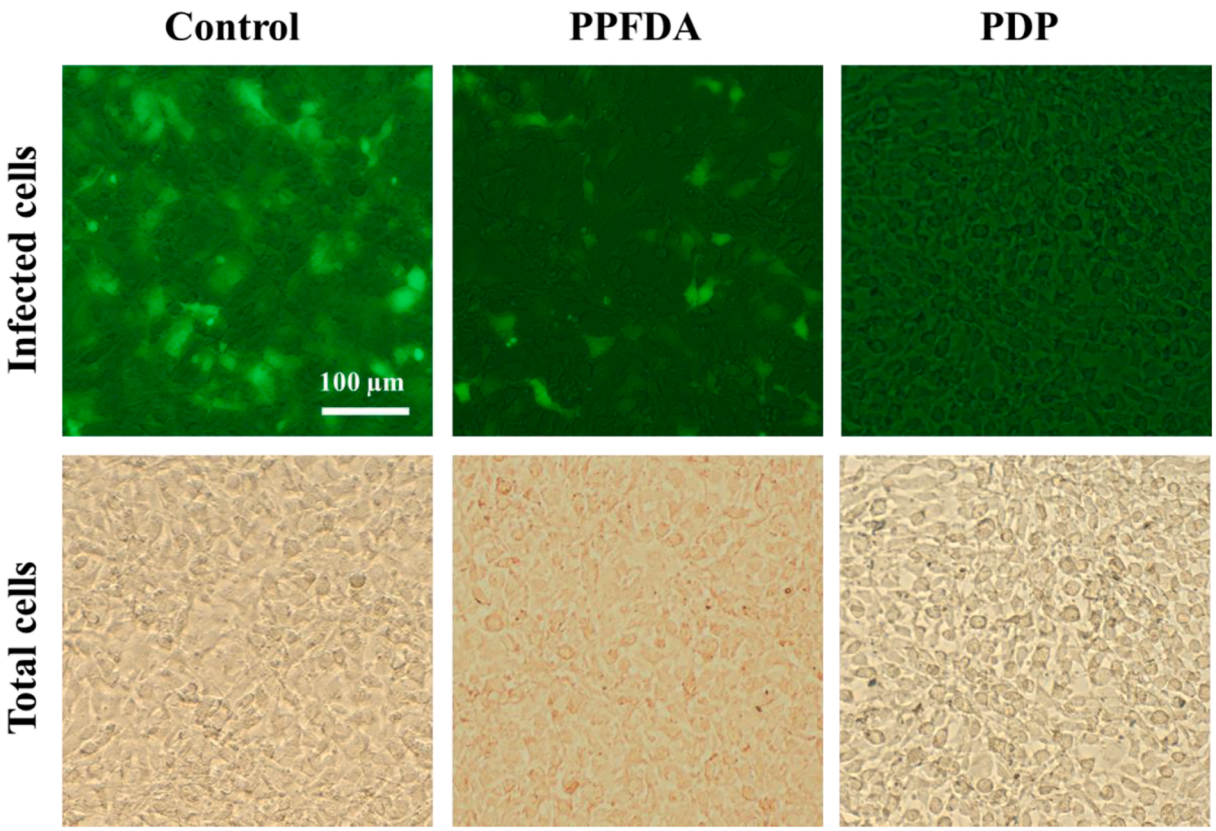

Fig. 8. Antiviral activity of PPFDA and PDP coated textiles against lentivirus-EGFP. The virus-infected cells are in green fluorescence, indicating sample cannot inactivate viruses; the cells without green fluorescence demonstrating an excellent virucidal activity of PDP coated textile. The total cells are observed in bright field for comparison.

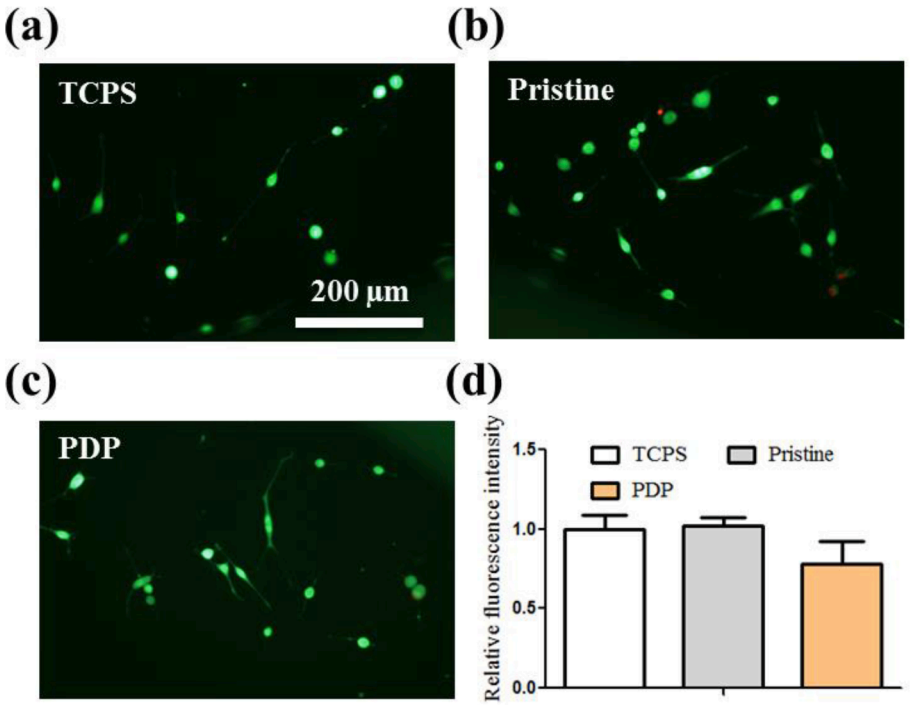

Fig. 9. *In vitro* biocompatibility toward mouse fibroblast NIH3T3 cells. LIVE/DEAD fluorescent images of cells in three groups: (a) TCPS control, (b) pristine textile, and (c) PDP coated textile. (d) Cell proliferation in three groups determined by Alamar Blue assay.

3.6. Biocompatibility

The biocompatibility of PDP toward mouse NIH 3T3 fibroblast cells was investigated after 24 h of incubation *in vitro*. The cell viability was determined with LIVE/DEAD assay presented in Fig. 9a-c, and there is no obvious difference in cell morphology on TCPS control, pristine textile, and PDP coated textile. The cellular metabolic activity after treatment with samples was measured using Alamar Blue (10% v/v) assay, and the relative fluorescence intensities in TCPS control, pristine textile, and PDP coated textile groups are not significantly different ($P > 0.05$, Fig. 9d) and the values were 1.00 ± 0.16, 1.02 ± 0.10, and 0.78 ± 0.25, respectively. The above results demonstrated that the biocompatibility of PDP coated textile was as good as TCPS and pristine textile *in vitro*.

4. Conclusions

In this study, a fluorinated polycationic coating P(DMAMS-*co*-PFDA) (PDP) on the polyester textile was synthesized via one-step iCVD. EDX and FTIR verified the chemical compositions of the coating. The contact angle analysis demonstrated that the PDP coating converted the surface of polyester textile from hydrophilic to hydrophobic, from oleophilic to oleophobic, which endowed the surface with effective antifouling activity against the liquid attachment, such as blood, paraffin oil, honey, milk, etc. The zeta potential data showed that the PDP coating endowed the polyester textile with a positively charged surface, and the bacteria and virus in this study were negatively charged. When the external force enabled the bacteria and viruses to attach onto the textile surface, PDP coating exhibited excellent antimicrobial activity against gram-negative *E. coli*, gram-positive drug-resistant MRSA, and lentivirus-EGFP, which was primarily due to the electrostatic interaction between the negatively charged microbes and cationic PDP. The PDP coating showed good biocompatibility toward mouse NIH 3T3 fibroblast cells. Taken together, PDP as a hydrophobic polycationic coating with broad-spectrum antimicrobial activity would have promising prophylactic applications to control the bacterial and viral infections.

Declaration of Competing Interest

The authors declare that they have no known competing financial interests or personal relationships that could have appeared to influence the work reported in this paper.

Acknowledgements

We are grateful for the funding supports from Ningbo Natural Science Foundation (202003N4050), the National Natural Science Foundation of China (21706222, 52073230, 21875189, 31701523, and 32072969), the open research fund of Key Laboratory for Organic Electronics and Information Displays, the Joint Research Funds of Department of Science & Technology of Shaanxi Province and Northwestern Polytechnical University (No. 2020GXLH-Z-021 and 2020GXLH-Z-013), and the Fundamental Research Funds for the Central Universities, China. We would like to thank the Analytical & Testing Center of Northwestern Polytechnical University for the SEM and EDX tests.

References

[1] E.D. Brown, G.D. Wright, Antibacterial drug discovery in the resistance era, Nature 529 (7586) (2016) 336–343, https://doi.org/10.1038/nature17042.
[2] Q. Jia, Q. Song, P. Li, W. Huang, Rejuvenated Photodynamic Therapy for Bacterial Infections, Adv. Healthc. Mater. 8 (14) (2019), 1900608, https://doi.org/10.1002/adhm.201900608.
[3] A.P. Magiorakos, A. Srinivasan, R.B. Carey, Y. Carmeli, M.E. Falagas, C.G. Giske, S. Harbarth, J.F. Hindler, G. Kahlmeter, B. Olsson-Liljequist, D.L. Paterson, L. B. Rice, J. Stelling, M.J. Struelens, A. Vatopoulos, J.T. Weber, D.L. Monnet, Multidrug-resistant, extensively drug-resistant and pandrug-resistant bacteria: an international expert proposal for interim standard definitions for acquired resistance, Clin. Microbiol. Infect. 18 (3) (2012) 268–281, https://doi.org/10.1111/j.1469-0691.2011.03570.x.
[4] R. Li, J. Dou, Q. Jiang, J. Li, Z. Xie, J. Liang, X. Ren, Preparation and antimicrobial activity of β-cyclodextrin derivative copolymers/cellulose acetate nanofibers, Chem. Eng. J. 248 (2014) 264–272, https://doi.org/10.1016/j.cej.2014.03.042.
[5] G.A. Tannock, H. Kim, L. Xue, Why are vaccines against many human viral diseases still unavailable; an historic perspective? J. Med. Virol. 92 (2) (2020) 129–138, https://doi.org/10.1002/jmv.25593.
[6] Z. Shang, S.Y. Chan, W.J. Liu, P. Li, W. Huang, Recent Insights into Emerging Coronavirus: SARS-CoV-2, ACS Infect. Dis. (2020), https://doi.org/10.1021/acsinfecdis.0c00646.
[7] Q. Jiang, L. Lu, COVID-19: From crude oil to medical mask, ES Mater. Manuf. (2020), https://doi.org/10.30919/esmm5f766.
[8] P. Tsai, Performance of masks and discussion of the inactivation of SARS-CoV-2, Eng. Sci. (2020), https://doi.org/10.30919/es8d1110.
[9] V.S. Shaikh, G.M. Nazeruddin, Y.I. Shaikh, S.H. Bloukh, Z. Edis, H.M. Pathan, A recapitulation of virology, modes of dissemination, diagnosis, treatment, and preventive measures of COVID-19: A review, Eng. Sci. 10 (2020) 11–23, https://doi.org/10.30919/es8d1009.
[10] Y.I. Shaikh, V.S. Shaikh, K. Ahmed, G.M. Nazeruddin, H.M. Pathan, The revelation of various compounds found in Nigella sativa L. (Black Cumin) and their possibility to inhibit COVID-19 infection based on the molecular docking and physical properties, Eng. Sci. 11 (2020) 31–35, https://doi.org/10.30919/es8d1127.
[11] V.S. Shaikh, Y.I. Shaikh, K. Ahmed, A. Sagar, A molecular docking study of lopinavir towards SARS-COV-2 target protein, Eng. Sci. 12 (2020) 113–118, https://doi.org/10.30919/es8d1226.
[12] F. Siedenbiedel, J.C. Tiller, Antimicrobial Polymers in Solution and on Surfaces: Overview and functional principles, Polymers 4 (1) (2012) 46–71, https://doi.org/10.3390/polym4010046.
[13] Y. Su, T. Feng, W. Feng, Y. Pei, Z. Li, J. Huo, C. Xie, X. Qu, P. Li, W. Huang, Mussel-inspired, surface-attachable initiator for grafting of antimicrobial and antifouling hydrogels, Macromol. Rapid Commun. 40 (17) (2019), 1900268, https://doi.org/10.1002/marc.201900268.
[14] Q. Gao, P. Li, H. Zhao, Y. Chen, L. Jiang, P.X. Ma, Methacrylate-ended polypeptides and polypeptoids for antimicrobial and antifouling coatings, Polym. Chem. 8 (41) (2017) 6386–6397, https://doi.org/10.1039/C7PY01495C.
[15] Y. Zou, Y. Zhang, Q. Yu, H. Chen, Dual-function antibacterial surfaces to resist and kill bacteria: Painting a picture with two brushes simultaneously, J. Mater. Sci. Technol. 70 (2021) 24–38, https://doi.org/10.1016/j.jmst.2020.07.028.
[16] X. Ding, S. Duan, X. Ding, R. Liu, F.-J. Xu, Versatile antibacterial materials: An emerging arsenal for combatting bacterial pathogens, Adv. Funct. Mater. 28 (40) (2018), 1802140, https://doi.org/10.1002/adfm.201802140.
[17] S. Zhang, X. Yang, B. Tang, L. Yuan, K. Wang, X. Liu, X. Zhu, J. Li, Z. Ge, S. Chen, New insights into synergistic antimicrobial and antifouling cotton fabrics via dually finished with quaternary ammonium salt and zwitterionic sulfobetaine, Chem. Eng. J. 336 (2018) 123–132, https://doi.org/10.1016/j.cej.2017.10.168.
[18] K. Zhu, J. Zhang, H. Zhang, H. Tan, W. Zhang, Y. Liu, H. Zhang, Q. Zhang, Fabrication of durable superhydrophobic coatings based on a novel branched fluorinated epoxy, Chem. Eng. J. 351 (2018) 569–578, https://doi.org/10.1016/j.cej.2018.06.116.
[19] H. Liu, J. Huang, Z. Chen, G. Chen, K.-Q. Zhang, S.S. Al-Deyab, Y. Lai, Robust translucent superhydrophobic PDMS/PMMA film by facile one-step spray for self-cleaning and efficient emulsion separation, Chem. Eng. J. 330 (2017) 26–35, https://doi.org/10.1016/j.cej.2017.07.114.
[20] Q. Borjihan, J. Yang, Q. Song, L. Gao, M. Xu, T. Gao, W. Liu, P. Li, Q. Li, A. Dong, Povidone-iodine-functionalized fluorinated copolymers with dual-functional antibacterial and antifouling activities, Biomater. Sci. 7 (8) (2019) 3334–3347, https://doi.org/10.1039/C9BM00583H.
[21] P. Li, Y.F. Poon, W. Li, H.-Y. Zhu, S.H. Yeap, Y. Cao, X. Qi, C. Zhou, M. Lamrani, R. W. Beuerman, E.-T. Kang, Y. Mu, C.M. Li, M.W. Chang, S.S. Jan Leong, M.B. Chan-Park, A polycationic antimicrobial and biocompatible hydrogel with microbe membrane suctioning ability, Nat. Mater. 10 (2) (2011) 149–156, https://doi.org/10.1038/nmat2915.
[22] L. Mi, M.T. Bernards, G. Cheng, Q. Yu, S. Jiang, pH responsive properties of non-fouling mixed-charge polymer brushes based on quaternary amine and carboxylic acid monomers, Biomaterials 31 (10) (2010) 2919–2925, https://doi.org/10.1016/j.biomaterials.2009.12.038.
[23] B. Michen, T. Graule, Isoelectric points of viruses, J. Appl. Microbiol. 109 (2) (2010) 388–397, https://doi.org/10.1111/j.1365-2672.2010.04663.x.
[24] J. Haldar, A.K. Weight, A.M. Klibanov, Preparation, application and testing of permanent antibacterial and antiviral coatings, Nat. Protoc. 2 (10) (2007) 2412–2417, https://doi.org/10.1038/nprot.2007.353.
[25] Y. Jiao, L.-N. Niu, S. Ma, J. Li, F.R. Tay, J.-H. Chen, Quaternary ammonium-based biomedical materials: State-of-the-art, toxicological aspects and antimicrobial resistance, Prog. Polym. Sci. 71 (2017) 53–90, https://doi.org/10.1016/j.progpolymsci.2017.03.001.
[26] E. Çıtak, H. Testici, M. Gürsoy, E. Sevgili, H.T. Dağı, B. Öztürk, M. Karaman, Vapor deposition of quaternary ammonium methacrylate polymers with high antimicrobial activity: Synthetic route, toxicity assessment, and durability analysis, J. Vac. Sci. Technol., A 38 (4) (2020), 043203, https://doi.org/10.1116/1.5145285.
[27] C. Su, Y. Hu, Q. Song, Y. Ye, L. Gao, P. Li, T. Ye, Initiated chemical vapor deposition of graded polymer coatings enabling antibacterial, antifouling, and biocompatible surfaces, ACS Appl. Mater. Inter. 12 (16) (2020) 18978–18986, https://doi.org/10.1021/acsami.9b22611.

[28] J. Lin, X. Chen, C. Chen, J. Hu, C. Zhou, X. Cai, W. Wang, C. Zheng, P. Zhang, J. Cheng, Z. Guo, H. Liu, Durably antibacterial and bacterially antiadhesive cotton fabrics coated by cationic fluorinated polymers, ACS Appl. Mater. Inter. 10 (7) (2018) 6124–6136, https://doi.org/10.1021/acsami.7b16235.
[29] J. Haldar, D. An, L. Alvarez de Cienfuegos, J. Chen, A.M. Klibanov, Polymeric coatings that inactivate both influenza virus and pathogenic bacteria, Proc. Natl. Acad. Sci. 103 (47) (2006) 17667–17671, https://doi.org/10.1073/pnas.0608803103.
[30] D. Park, A.M. Larson, A.M. Klibanov, Y. Wang, Antiviral and Antibacterial Polyurethanes of Various Modalities, Appl. Biochem. Biotech. 169 (4) (2013) 1134–1146, https://doi.org/10.1007/s12010-012-9999-7.
[31] S.J. Yu, K. Pak, M.J. Kwak, M. Joo, B.J. Kim, M.S. Oh, J. Baek, H. Park, G. Choi, D. H. Kim, J. Choi, Y. Choi, J. Shin, H. Moon, E. Lee, S.G. Im, Initiated chemical vapor deposition: A versatile tool for various device applications, Adv. Eng. Mater. 20 (3) (2018) 1700622, https://doi.org/10.1002/adem.201700622.
[32] B. Zhi, Q. Song, Y. Mao, Vapor deposition of polyionic nanocoatings for reduction of microglia adhesion, RSC Adv. 8 (9) (2018) 4779–4785, https://doi.org/10.1039/C7RA12728F.
[33] N. Wu, Q. Hu, R. Wei, X. Mai, N. Naik, D. Pan, Z. Guo, Z. Shi, Review on the electromagnetic interference shielding properties of carbon based materials and their novel composites: Recent progress, challenges and prospects, Carbon 176 (2021) 88–105, https://doi.org/10.1016/j.carbon.2021.01.124.
[34] V. Elayappan, V. Murugadoss, Z. Fei, P.J. Dyson, S. Angaiah, Influence of polypyrrole incorporated Electrospun Poly(vinylidene fluoride-co-hexafluoropropylene) nanofibrous composite membrane electrolyte on the photovoltaic performance of dye sensitized solar cell, Eng. Sci. 10 (2020) 78–84, https://doi.org/10.30919/es5e1007.
[35] Y. Ye, Q. Song, Y. Mao, Single-step fabrication of non-leaching antibacterial surfaces using vapor crosslinking, J. Mater. Chem. 21 (1) (2011) 257–262, https://doi.org/10.1039/C0JM02578J.
[36] Y.Y. Smolin, S. Janakiraman, M. Soroush, K.K.S. Lau, Experimental and theoretical investigation of dye sensitized solar cells integrated with crosslinked poly (vinylpyrrolidone) polymer electrolyte using initiated chemical vapor deposition, Thin Solid Films 635 (2017) 9–16, https://doi.org/10.1016/j.tsf.2016.12.034.
[37] Y. Ye, Q. Song, Y. Mao, Solventless hybrid grafting of antimicrobial polymers for self-sterilizing surfaces, J. Mater. Chem. 21 (35) (2011) 13188–13194, https://doi.org/10.1039/C1JM12050F.
[38] M. Gupta, K.K. Gleason, Initiated chemical vapor deposition of poly(1H,1H,2H,2H-perfluorodecyl Acrylate) thin films, Langmuir 22 (24) (2006) 10047–10052, https://doi.org/10.1021/la061904m.
[39] A.S. Anjum, K.C. Sun, M. Ali, R. Riaz, S.H. Jeong, Fabrication of coral-reef structured nano silica for self-cleaning and super-hydrophobic textile applications, Chem. Eng. J. 401 (2020), 125859, https://doi.org/10.1016/j.cej.2020.125859.
[40] Z.-S. Huang, Y.-Y. Quan, J.-J. Mao, Y.-L. Wang, Y. Lai, J. Zheng, Z. Chen, K. Wei, H. Li, Multifunctional superhydrophobic composite materials with remarkable mechanochemical robustness, stain repellency, oil-water separation and sound-absorption properties, Chem. Eng. J. 358 (2019) 1610–1619, https://doi.org/10.1016/j.cej.2018.10.123.
[41] K. Ellinas, K. Tsougeni, P.S. Petrou, G. Boulousis, D. Tsoukleris, E. Pavlatou, A. Tserepi, S.E. Kakabakos, E. Gogolides, Three-dimensional plasma micro–nanotextured cyclo-olefin-polymer surfaces for biomolecule immobilization and environmentally stable superhydrophobic and superoleophobic behavior, Chem. Eng. J. 300 (2016) 394–403, https://doi.org/10.1016/j.cej.2016.04.137.
[42] T.P. Martin, K.K. Gleason, Combinatorial Initiated CVD for Polymeric Thin Films, Chem. Vap. Depos. 12 (11) (2006) 685–691, https://doi.org/10.1002/cvde.200606495.
[43] D.D. Iarikov, M. Kargar, A. Sahari, L. Russel, K.T. Gause, B. Behkam, W.A. Ducker, Antimicrobial surfaces using covalently bound polyallylamine, Biomacromolecules 15 (1) (2014) 169–176, https://doi.org/10.1021/bm401440h.
[44] G. Choi, G.M. Jeong, M.S. Oh, M. Joo, S.G. Im, K.J. Jeong, E. Lee, Robust thin film surface with a selective antibacterial property enabled via a cross-linked ionic polymer coating for infection-resistant medical applications, ACS Biomater. Sci. Eng. 4 (7) (2018) 2614–2622, https://doi.org/10.1021/acsbiomaterials.8b00241.
[45] A.C. Engler, N. Wiradharma, Z.Y. Ong, D.J. Coady, J.L. Hedrick, Y.-Y. Yang, Emerging trends in macromolecular antimicrobials to fight multi-drug-resistant infections, Nano Today 7 (3) (2012) 201–222, https://doi.org/10.1016/j.nantod.2012.04.003.
[46] Y. Xue, H. Xiao, Antibacterial/antiviral property and mechanism of dual-functional quaternized pyridinium-type copolymer, Polymers 7 (11) (2015), https://doi.org/10.3390/polym7111514.
[47] C.T. Barrett, R.E. Dutch, Viral membrane fusion and the transmembrane domain, Viruses 12 (7) (2020), 693, https://doi.org/10.3390/v12070693.
[48] A.M. Larson, H.S. Oh, D.M. Knipe, A.M. Klibanov, Decreasing herpes simplex viral infectivity in solution by surface-immobilized and suspended N,N-Dodecyl,methyl-polyethylenimine, Pharm. Res. 30 (1) (2013) 25–31, https://doi.org/10.1007/s11095-012-0825-2.
[49] B.B. Hsu, S. Yinn Wong, P.T. Hammond, J. Chen, A.M. Klibanov, Mechanism of inactivation of influenza viruses by immobilized hydrophobic polycations, Proc. Natl. Acad. Sci. USA 108 (1) (2011) 61–66, https://doi.org/10.1073/pnas.1017012108.